Digest Journal of Nanomaterials and Biostructures Vol. 12, No. 3, July - September 2017, p. 719 - 726

LOW COST SYNTHESIS OF ZnO NANO THIN FILMS BY ELECTROCHEMICAL DEPOSITION

O. N. SALMAN[a], M. O. DAWOOD[b] A. K. ALI[a], D. S. AHMED[a*], K. I. HASSOON[a]
[a]*Department of Applied Sciences, University of Technology, Baghdad, Iraq*
[b]*Physics Department, Almustansiriyah University, Baghdad, Iraq*

In this work, a simple electrochemical cell is used to deposit ZnO nano thin films (NTFs) onto ITO conductive substrates for three deposition times (5, 10, 15 min.) The produced films have transmission more than (80 %) for wavelengths above 600nm and high energy bandgap (3.6 -3.75 eV.) The measurements of the photoluminescence (PL) spectra revealed a sharp peak at 325 nm and a small peak at 675 nm. The XRD analysis demonstrated that the ZnO NTFs exhibited polycrystalline structure. The FE-SEM illustrates that the nominal diameter of particles is between 50 to 100 nm and that the nano-films are deposited uniformly on ITO substrate for deposition time 10 min. The energy dispersive X-ray (EDX) results revealed that only Zn2+ and O2- ions are available in the samples, indicating a pure ZnO composition. ZnO NTFs was used to prepare a dye sensitized solar cell (DSSC) with conversion efficiency 2.7 %.

(Received April 12, 2017; Accepted July 26, 2017)

Keyword: ECD, ZnO nanoparticles, XRD, AFM, FE-SEM

1. Introduction

In the last decade, there was a trend to use low cost method to prepare nano thin films for the applications of renewable energy devices [1-3]. ZnO and TiO_2 are among the most used materials to fabricate an important type of these devices called dye sensitized solar cell [4]. ZnO as a material has found numerous applications in many fields: for example it used as piezoelectric and optoelectronic device, in the area of electronics as field emitters, in lasers as medium for UV radiation, in industrial chemistry as photocatalysts [5-8]. However, the most interesting modern applications of ZnO is as an electron transport material in thin film and dye sensitized solar cell (DSSC) [9-11], polymer (or organic) solar cell [12,13], perovskite solar cell [14-16] and in general heterojunctions solar cell [17,18]. Many methods and techniques have been applied for the synthesis of zinc zxide nano thin films (ZnO NTFs), including magnetron sputtering [19], chemical vapor deposition [20], sol-gel processes [21], thermal evaporation [22] pulsed laser ablation (PLA) in some liquids [23], and molecular beam epitaxy [24].

Besides, the growth of well-aligned ZnO nanorods by chemical growth route was reported by Harnack et al. [25]. Most of the above methods are either costly or taking a long preparation time. Here in, we report electrochemical deposition (ECD) as a fast and low cost method, highly reproducible and compatible with a large area processing and it can facilitate uniform growth at low temperature aqueous solution [25].

The ECD technique used a quite low cathode voltage or current to produce a pure ZnO NTFs on any transparent conductive oxide-substrate such as Indium Tin Oxide (ITO) or Fluorine Tin Oxide (FTO) [26]. In the ECD, the film thickness, morphology and optical properties can be modified by various operating parameters namely: current density, applied potential, deposition time and the electrolyte concentration. Generally, in the deposition experiments, zinc nitrate solutions or zinc chloride solutions [27] are used as a precursor. The aim of this work is to

*Corresponding author: duhasaadi2015@gmail.com

obtain low cost ZnO NTFs using a simple technique and to investigate the potential of these films as an active layer in DSSC.

2. Experimental part

In this research the ECD cell is a simple homemade container made from Teflon with cylindrical shape of 9.5 cm internal radius, and 3.6 cm external radius. The distance between electrodes is 2cm. The anode and cathode material are Zn foil and ITO substrates; respectively. The ECD of the NTFs is carried out in that cell after putting 100 ml of 1mM from $Zn(NO_3)_2.5H2O$ at a constant temperature (35^oC). The pH of the electrolyte solution was fixed at 7.5. Deposition of the NTFs is implemented cathodically by using a power supply with a standard two electrodes system. The voltage between the two electrodes was 17.5 volt. ITO glasses of 2cm2 area and resistance 15 Ω/square from Cris Baker. ITO is used here as transparent electrode. In all our experiments, we fixed the current at 5mA and three deposition times (5, 10, 15 min.) The electrolyte precursor $Zn(NO_3)_2.5H2O$ was used in all the experiments. After the deposition process, the NTFs were annealed at 500^oC to obtain best adhesion with their ITO substrates.

In the deposition of ZnO, the hydroxide-ions are generated by the process of cathodic reduction of an oxygen precursor at the electrode surface which finally leads to the formation of ZnO. The three types of oxygen precursors have been discussed by Canava and Lincot [28]. The use of nitrate ions as the oxygen precursor has recently been reported as an alternative method for the ECD of ZnO NTFs.

The process of ECD for ZnO is clearly described by Yoshida et al. [29] and Kathalingam et al. [30]. The spectroscopic measurements and FE-SEM analyses are implemented using TC60 spectrophotometer and ZEISS equipment; respectively. In order to fabricate DSSC from ZnO NTFs, the ZnO/ITO electrode was immersed in an organic dye (N719 from DyeSol) for 24 hour and then annealed at 500 ^oC for 30 min. The rest of DSSC fabrication steps are analogous to the standards. Figure 1 shows a schematic diagram for DSSC with ZnO layer prepared by ECD (c.f. inset (a) of Fig. 7). The characterization of our solar cell is implemented using Halogen lamp which is simulated to give about 0.5 AM1 in the lab conditions.

3. Result and discussion

Transmittance spectral data of ZnO NTFs are obtained in the wavelength range (200−900) nm. Fig. (1a) shows the transmittance spectra of ZnO NTFs electrodeposited under three deposition times (5, 10, 15) min. All the spectra showed similar trends of transmittance variation, and all of them revealed high optical transmission values (about 80 %) above 600nm range for films of thickness about 600 nm which had a tendency to decrease with increasing thickness. The absorption edge is slightly green shifted with increasing of deposition time and this may be due to improved crystalline quality of the ZnO films growth. Fig. (1b) shows the $(\alpha h\nu)^2 - h\nu$ plot for ZnO films, where α is the absorption coefficient, h is Plank's constant and ν is the frequency of the incident light. The bandgap E_g of ZnO has been obtained by extension of the linear part of $(\alpha h\nu)^2$ to intercept with $h\nu$-axis. The optical bandgaps of the films is calculated using the well-known relation for direct transition

$$\alpha h\nu = C(h\nu - E_g)^{1/2} \tag{1}$$

where C is a constant, $h\nu$ is the photon energy. The E_g value calculated from the extrapolation method was in the range from 3.6 eV to 3.75 eV for the deposition time of 5 min and 10 min, respectively. This illustrates that bandgap of ZnO can be rather tailored. The bulk bandgap of ZnO has a nominal value of 3.37eV. However we obtained higher values in the range of 3.6 to

3.7 eV for ZnO prepared by ECD in our experimental conditions. Another group [25], who also prepared ZnO by ECD but using different experimental conditions, obtained two values (3.36 and 3.41eV) for direct E_g. This discrepancy can be ascribed to the intrinsic defects [27] and quantum size effects [25].

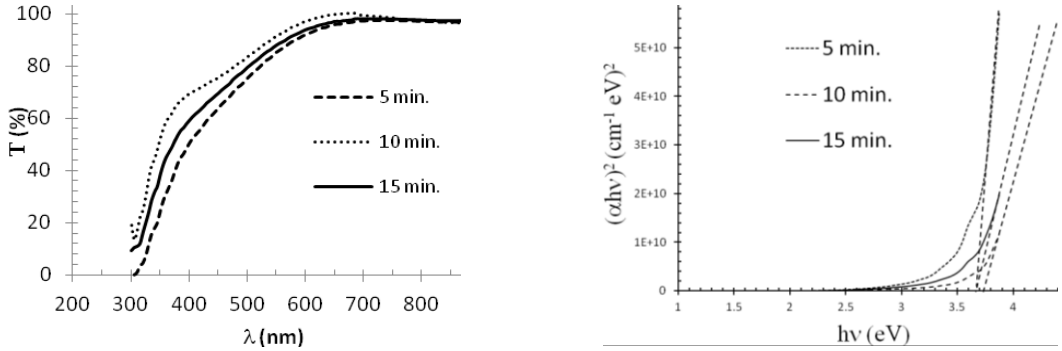

Fig. 1. The transmittance a) and the bandgaps b) for ZnO films prepared by ECD for three depositions times

For further study of the PL-spectra of such ZnO films, PL excitation and time resolved PL spectra are also measured. Figure (2) is obtained at excitation wavelength of 325 nm. We only detected a relatively weak and broad visible emission around 675nm for the three deposition times. The energy bandgap from photoluminescence spectrum of the ZnO film is calculated by using Plank's law:

$$E_g(eV) = 1240 / \lambda(nm) \tag{2}$$

where $E_g(eV)$ and $\lambda(nm)$ in Eqn. (2) indicates that the energy bandgap and the wavelength are in eV and nm units; respectively. At an excitation of 325nm, the peak UV emission around 325 nm is the strongest one at $E_g = 3.81\,eV$; the emission around 675 nm is a weak emission at $E_g = 1.83\,eV$. We can see a sharp excitonic absorption near the bandgap edge 325 nm, indicating that the main excitation mechanism for the UV emission is electron-hole pair by interband absorption.

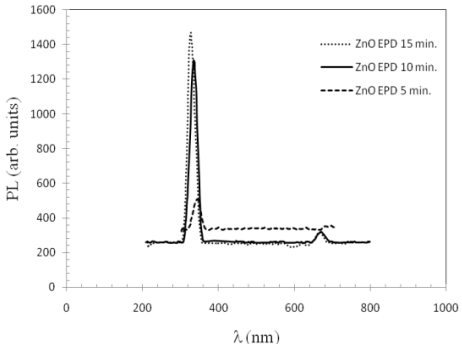

Fig. 2. PL spectrum for ZnO NTFs prepared by ECD

Table1. Value of (D, ε, δ) for ZnO NTFs prepared by ECD for 10 min.

hkl	2Θ(deg)	Beta(deg)	Grain size D (nm)	(ε) Strain×10^{-4} (lines^2/m^4)	(D) Dislocation ×10^{14} (1/m^2)
(100)	30.4926	0.34	84.96	14.38	1.38
(002)	35.2959	0.3767	77.65	15.73	1.65

The XRD pattern of ZnO NTFs on the ITO glass substrate proved that the film exhibited a polycrystalline nature and the resulted XRD pattern showed that ZnO NTFs had a hexagonal wurtzite structure [27]. Many researchers have reported that the most intense peak in the XRD-pattern was along the (100) plane and the ZnO NTFs was growing parallel to the c-axis of the hexagonal crystal structure. The full width at half maximum for each peak is small, revealing a good crystallization conditions with a large grain size. Assuming a homogeneous strain across crystallites, the size of nanocrystallines can be estimated from the full width half maximum (FWHM) values of diffraction peaks. The particle size could be obtained using Scherrer formula [6]:

$$D = \frac{K\lambda}{\beta_{2\theta}\cos\theta} \tag{2}$$

where K is a constant often approximated to 0.94, ($\lambda = 1.54$ Å) is the X-ray wavelength, 2θ the Bragg angle and $\beta_{2\theta}$ is the FWHM of the diffraction peak. A grain size value of 77.65nm crystallite size has been estimated from (002) diffraction peak for ZnO films electrodeposited. Though several phases of ZnO are observed, especially two phases at ZnO (100) at 30.492° and ZnO (002) at 35.295° are dominant on the ITO substrate. The dislocation density $\delta = 1/D^2$ and micro-strain $\varepsilon = (\beta_{2\theta}\cos\theta)/4$ were calculated in Table (1) following reference [28].

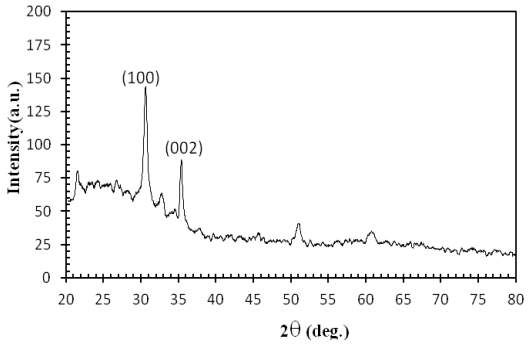

Fig. 3. XRD for ZnO NTFs prepared by ECD for 10 min.

The surface morphologies of the grown structures are observed by the AFM investigations and the images are shown in Fig. (4). The result show that the different deposition times used in the preparation of ZnO NTFs. Times strongly affect of the surface NTFs. The surface grain size, roughness and RMS values are presented in Table (2).

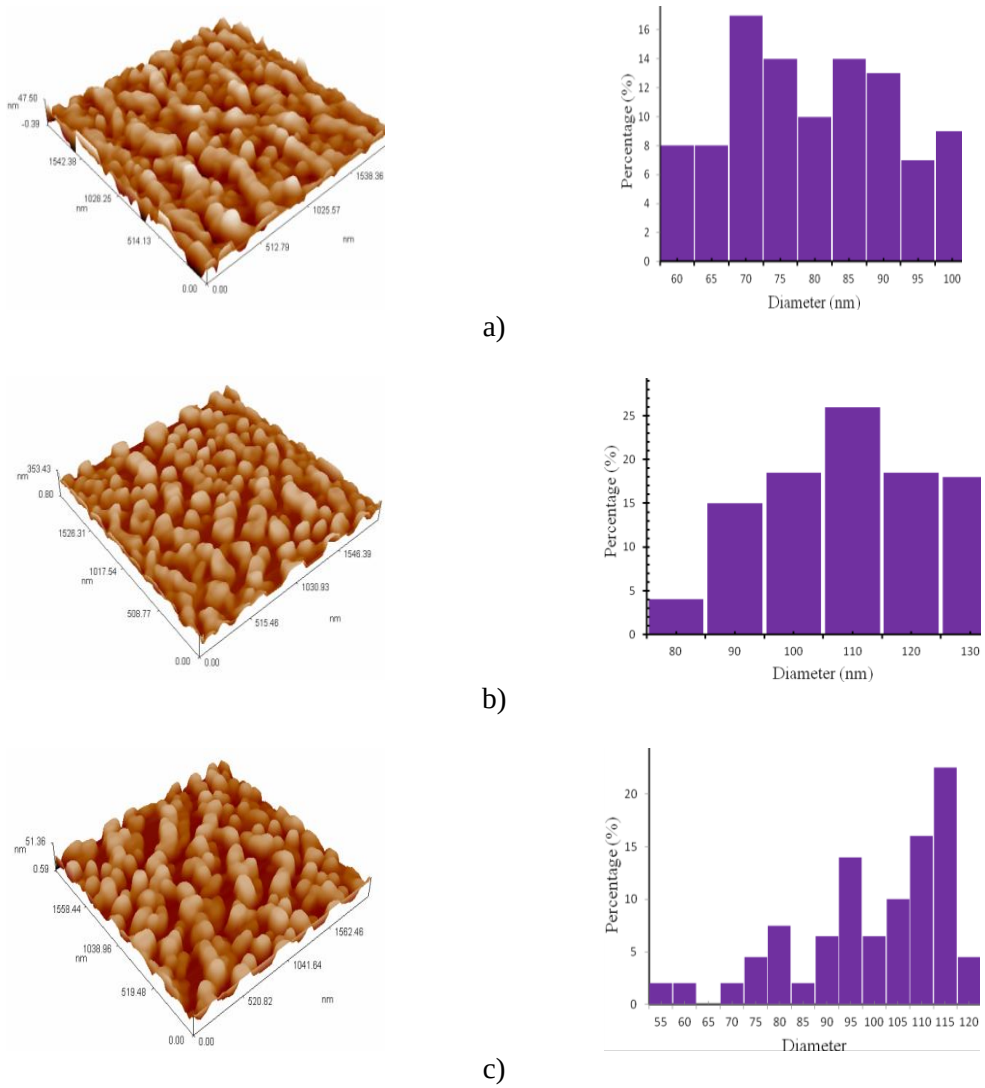

Fig. 4. AFM images for ZnO NTFs prepared by ECD for : (a) 5 min, (b) 10 min, and (c) 15 min.

Table 2. Average values of grain size, roughness and RMS extracted from AFM measurements.

Deposition time (min)	Average Grain size(nm)	Average Roughness (nm)	RMS
5	77.15	6.23	7.61
10	96.57	7.28	8.39
15	104.6	47.1	54.2

The obtained FE-SEM images show that all the ZnO NTFs consist of nanoparticles with diameters in the range (55-130 nm). This is compatible with AFM analyses in Fig. (4). The different degrees of brightness of the grains indicate the presence of multiple layers of ZnO on the substrates. The brighter grains represent the upper layer of the NTFs and the darker grains represent the lower layer of the NTFs. These FE-SEM images are similar to that of [29] which prepared by SILAR technique. The shapes of ZnO nanocrystals are spherical obviously demonstrate in Figure (5). The EDX study of the prepared sample is shown in Fig. (6). It shows that the sample contains only Zinc and Oxygen and small proportions of other metals.

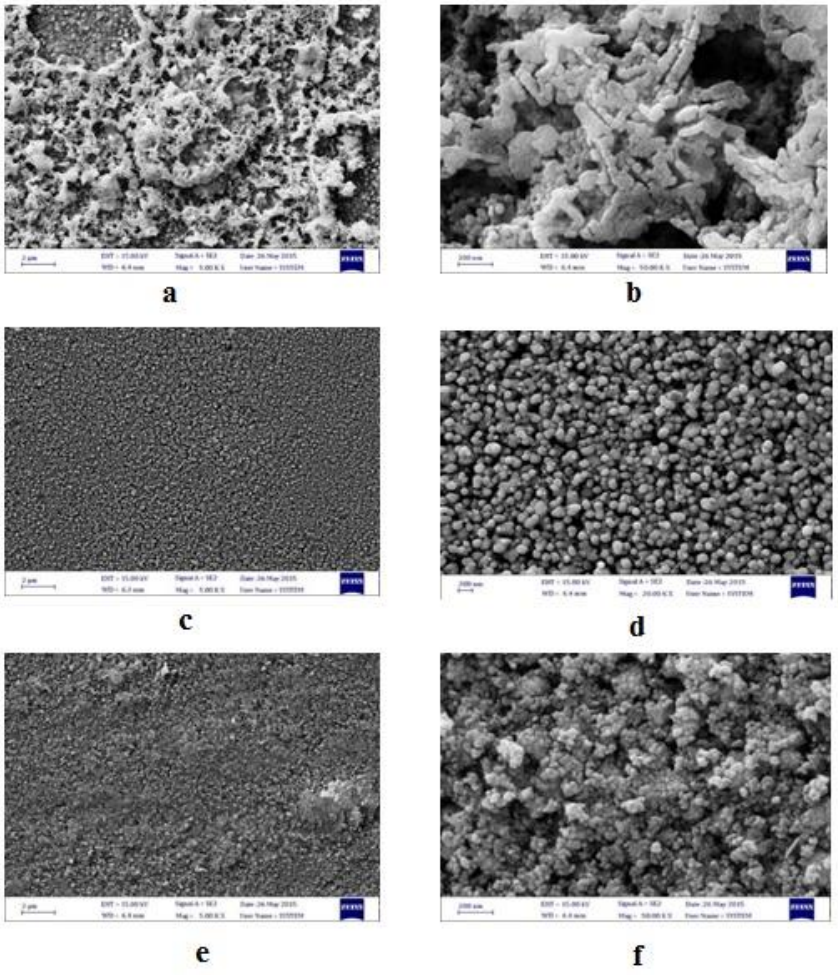

Fig. 5. FE-SEM for ZnO NTF fabricated by ECD technique for the following deposition time and the corresponding white bar length respectively: (a) 5 min, 2 μm, (b) 5 min, 200 nm (c) 10 min, 2 μm, (d) 10 min, 200 nm, (e) 15 min, 2 μm, (f) 15 min, 200 nm.

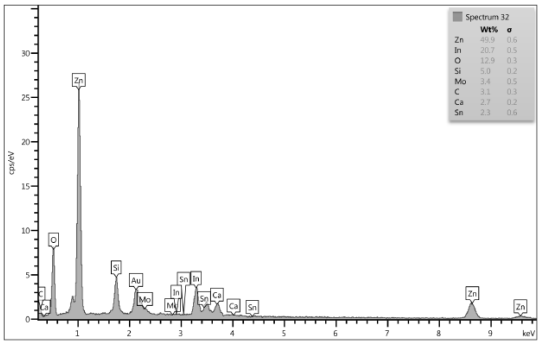

Fig. 6. EDX for ZnO thin films deposited in 10 min

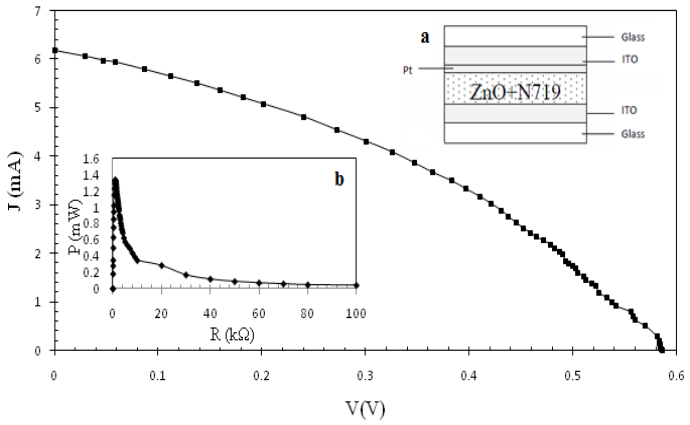

Fig. 7. Charactersitics of DSSCs with ZnO active layer prepared by ECD. Inset (a) Structure of DSSC. Inset (b) The is the output power for different load resistance

Fig. 7 shows J-V characteristics of DSSCs with ZnO layer prepared by ECD for different load resistance. The applied input power density is 50 mW/cm^2 which is about half of AM1. Maximum output power density is 1.34 mW/cm^2 which corresponds to conversion efficiency. 2.68 %. Table 2 summarizes the results. Although the efficiency of that DSSCs is still not competitor to other types of solar cells, we still need such a low cost solar cells with acceptable conversion efficiency.

Table 3. Solar cell parameters for DSSC with ZnO layer prepared by ECD

V_{oc} (V)	J_{sc} (mA)	V_m (V)	J_m (mA)	Rs (Ω)	Rsh (kΩ)	F.F	η (%)
0.59	6.17	0.35	3.86	25.0	17.1	0.37	2.7

4. Conclusions

In this study, we report a successful synthesis of low cost ZnO NTFs by using a simple ECD cell with a relatively low d.c potential of 17.5 volt applied between two electrical electrodes immersed in a tenuous zinc nitrate aqueous solution at room temperature. The morphological images have shown that different deposition times in minute have a great effect on the physical parameters of the grown structures.

However, it has been observed that the values of the direct bandgaps prepared by ECD were relatively high and they were almost the same for the three different times. XRD studies revealed that the deposited films were polycrystalline in nature with wurtzite phase. The NTFs ZnO prepared by ECD can be used to fabricate DSSC with acceptable conversion efficiency.

References

[1] C. Florica, A. Costas, A. Kuncser, N. Preda, I. Enculescu, Nanotechnology **28**, 27 (2016) .
[2] Z. Lin,j. . Wang, Springer-Technology and Engineering, (2014).
[3] L. Wei, Q. Liu, B. Zhu, W. Liu, S. Ding , H. Lu, A. Jiang and D. W. Zhang, Nanoscale Research Letters **11**, 213 (2016).
[4] C. Xu, J. Wu, U. V. Desai, D. Gao, Nano Lett. **12**(5), 2420 (2012).
[5] P. Yang, H. Yan, S. Mao, R. Russo, J. Johnson, R. Saykally, N. Morris, J. Pham, R. He, H. J. Choi, Adv. Funct. Mater. **12**, 323 (2002).
[6] S. Chen, J. Zbang, X. Feng, X. Wang, L. Luo, Y. Shi, O.Xue, C. wang J. Zhu, Z. Zhu, Appl. Surf. Sci. **241**, 384 (2005).
[7] L. Luo, Y. Zhang, S.S. Mao, L. Lin, A Phys. **127**, 201 (2006).

[8] Y.W. Zhu, H.Z. Zhang, X.C. Sun, S.Q. Feng, J. Xu, Q. Zhao, B. Xiang, R. M. Wang, Appl. Phys. Lett. **83**, 144 (2003).
[9] T. Loewenstein, K. Nonomura, T. Yoshida, E. Michaelis, D. Wöhrle, J. Rathousky, M.Wark D. Schlettwein, J. Electrochem. Soc., **153,** A699 (2006).
[10] K. Keis, E. Magnusson, H. Lindström, S.-E. Lindquist, A. Hagfeldt, Solar Energy Materials and Solar Cells **73**(1), 51 (2002).
[11] Q. Zhang, C. S. Dandeneau, X. Zhou, G. Cao, Adv. Mater. **21**, 4087 (2009)
[12] J. B. You, C. C. Chen, L. T. Dou, S. Murase, H. S. Duan, S. A. Hawks, T. Xu, H. J. Son, L. P. Yu, G. Li, Adv. Mater. **24**, 5267 (2012).
[13] Hin-Lap Yip, S. K. Hau, N. S. Baek, H. Ma, A. K.-Y. Jen Adv. Mater. **20**, 2376 (2008).
[14] D.-Y. Son, J.-H. Im, H.-S. Kim, N.-G. Park, J. Phys. Chem. C **118**(30), 16567 (2014).
[15] M. H. Kumar, N. Yantara, S. Dharani, M. Graetzel, S. Mhaisalkar, P. P. Boix, N. Mathews, Chem. Commun. **49**, 11089 (2013).
[16] D. Liu, T. L. Kelly, Nat. Photon **8**, 133 (2014).
[17] T. Minami, Y. Nishi, T. Miyata, J. Nomoto, Applied Physics Express 4 (2011) 062301.
[18] J. M. Luther, J. Gao, M. T. Lloyd, O. E. Semonin, M. C. Beard, Arthur J. Nozik **22**(33), 3704 (2010).
[19] C. L. Hsu, S. J. Chang, Y. R. Lin, P. C. Li, T. S. Lin, S. Y. Tsai, et al., Chemical Physics Letters **416**, 75 (2005).
[20] D. Barreca, D. Bekermann, E. Comini, A. Devi, R. A. Fischer, A. Gasparotto, et al., Sensors and Actuators B: Chemical **149**, 1 (2010).
[21] C. Zhang, Journal of Physics and Chemistry of Solids **71**, 364 (2010).
[22] J. H. Zheng, Q. Jiang, J. S. Lian, Applied Surface Science **257**, 5083 (2011).
[23] Raid A. Ismail, Abdulrahman K. Ali , Mukhlis M. Ismail, Khaleel I. Hassoon, Appl. Nanosci. **1**, 45 (2011).
[24] D. C. Look, D. C. Reynolds, C. W. Litton, R. L. Jones, D. B. Eason, G. Cantwell, Applied Physics Letters **81**, 1830 (2002).
[25] O. Harnack, C. Pacholski, H. Weller, A. Yasuda, J. M. Wessels, Nano Letters **3**,1097 (2003).
[26] Y. Tak, K. Yong, The Journal of Physical Chemistry B **109**, 19263 (2005).
[27] J. Cembrero, A. Elmanouni, B. Hartiti, M. Mollar and B. Mari, Thin Solid Films **451-452**, 198 (2004) .
[28] B. Canava, D. Lincot, Journal of Applied Electrochemistry **30**, 711 (2000).
[29] T. Yoshida, T., D. Komatsu, N. Shimokawa, and H. Minoura, Thin Solid Films **451-452**, 166 (2004).
[30] A. Kathalingam, M. R. Kim, Y. S. Chae, J. K. Rhee, Journal of the Korean Physical Society **55**(6), 2476 (2009).